$\sqrt{2}\times\sqrt{2}$ structure and charge inhomogeneity at the surface of superconducting $BaFe_{2-x}Co_xAs_2$ ($x=0-0.32$)

Hui Zhang, Jun Dai, Yujing Zhang, Danru Qu, Huiwen Ji, G. Wu, X. F. Wang, X. H. Chen, Bing Wang, Changgan Zeng,* Jinlong Yang,† and J. G. Hou

Hefei National Laboratory for Physical Sciences at Microscale and Department of Physics, University of Science and Technology of China, 96 JinZhai Road, Hefei, Anhui 230026, China

(Received 10 December 2009; revised manuscript received 25 January 2010; published 18 March 2010)

The structure and electronic property at the cleaved (001) surfaces of the newly discovered pnictide superconductors $BaFe_{2-x}Co_xAs_2$ with x ranging from 0 to 0.32 are systematically investigated by scanning tunneling microscopy. A $\sqrt{2}\times\sqrt{2}$ surface structure is revealed to dominate for all the compounds and is identified to be Ba layer with half Ba atoms lifted off by combination with theoretical simulation. Charge inhomogeneity is observed at this $\sqrt{2}\times\sqrt{2}$ surface associated with an energy gap of about 30 meV for all the compounds.

DOI: 10.1103/PhysRevB.81.104520 PACS number(s): 74.25.Jb, 68.37.Ef, 74.50.+r, 74.62.Bf

I. INTRODUCTION

The lately discovered high-T_c superconductors based on iron pnictides have ignited intense research interests, following the cuprate boom.[1–7] Although progresses have been made to understand their structural, electronic, and magnetic properties, the nature of superconductivity is yet a mystery.[8] Among the experimental techniques used to investigate the high-T_c superconductors, surface-sensitive probes such as angle-resolved photoemission spectroscopy (ARPES) and scanning tunneling microscope (STM) have played a critical role due to their unrivaled energy and spatial/momentum resolution. However the surface might differ from the bulk structurally and electronically, due to the symmetry breaking and/or reconstruction. So thorough understanding of the surface structure and electronic properties at atomic scale is crucial to interpret correctly the experimental databased on surface-sensitive detections. On the other hand, the discrepant correlation between lattice, charge, and spin at the surface may lead to two-dimensional collective order, which would open a door to the nanoelectronics applications based on correlated materials.

STM has been used to investigate the 122-type pnictide compounds, for which high-quality single crystals can be grown.[6,7] Stripe[9–11] or square-lattice[12–14] structures were observed at the surfaces of some certain compounds. The latter was attributed to FeAs (Refs. 12 and 13) or 50% Ba (Ref. 14) terminations. So the surface termination of the 122-type pnictides is still unclear, and the evolution of the geometric and electronic structures as a function of doping level has never been explored at atomic scale. In this paper, we report systematic STM study of electron-doped 122 compounds ($BaFe_{2-x}Co_xAs_2$) with nominal doping composition of $x=0$, 0.08, 0.17, 0.20, 0.25, 0.32. A $\sqrt{2}\times\sqrt{2}$ surface structure is observed to prevail for all the doping levels. With the aid of theoretical simulation, this surface structure is determined to be well-ordered Ba plane with half Ba atoms lifted off. Strikingly, Electronic modulation with short-range order is characterized on such $\sqrt{2}\times\sqrt{2}$ surface for all the compounds accompanied by an energy gap around 30 meV.

II. EXPERIMENT

The growth of pnictide single crystals and their magnetic/transport characterization have been described elsewhere.[15] The crystals were cleaved *in situ* at ~120 K in ultrahigh vacuum environment with pressure lower than 2×10^{-10} mbar and immediately transferred into an Omicron STM stage, which were already cooled to 5 K. We examined one or two samples for each doping concentration. The same tungsten tip was used for all the STM characterization.

III. RESULTS AND DISCUSSION

The dominating surface for all the samples is atomically flat except for some defects or defect lines and a large-scale STM image for $x=0.20$ is shown in Fig. 1(a). When low bias and high current are adopted, square lattice with lattice constant of ~5.6 Å can be resolved on such surfaces, and the typical STM images with atomic resolution for $x=0$ and 0.20 are shown in Figs. 1(b) and 1(c). This square surface lattice dominates all the investigated compounds with Co concentration ranging from 0 to 0.32. It is quite striking, since the structure is orthorhombic for $x<0.20$ while tetragonal for $x>0.20$ at 5 K.[15] Occasionally, we also observed the stripe structure that was reported previously.[9–11] But it is rare in our case and has only been observed in compounds with $x=0$ and 0.20. Scanning tunneling spectroscopy (STS) measurement was also performed on such surfaces for all the investigated samples at 5 K, and the typical dI/dV spectroscopies taken away from defects are shown in Fig. 1(g). A protrusion feature at about −0.2 V is observed in the STSs for all the samples, which could originate from collective ordering or band-structure effect.

In the $BaFe_{2-x}Co_xAs_2$ compounds consisting of FeAs layers separated by a single Ba layer, the bond between Fe and As atoms is quite strong, so the cleavage is likely to happen between the FeAs layer and Ba layer, or in the Ba layer, leaving half of the Ba atoms on each exposed surfaces. The latter is more preferable energetically from theoretical calculation.[16] In order to determine the universally observed square surface structure, we did theoretical calculation with half layer of Ba atoms at the surface, which form $\sqrt{2}\times\sqrt{2}$

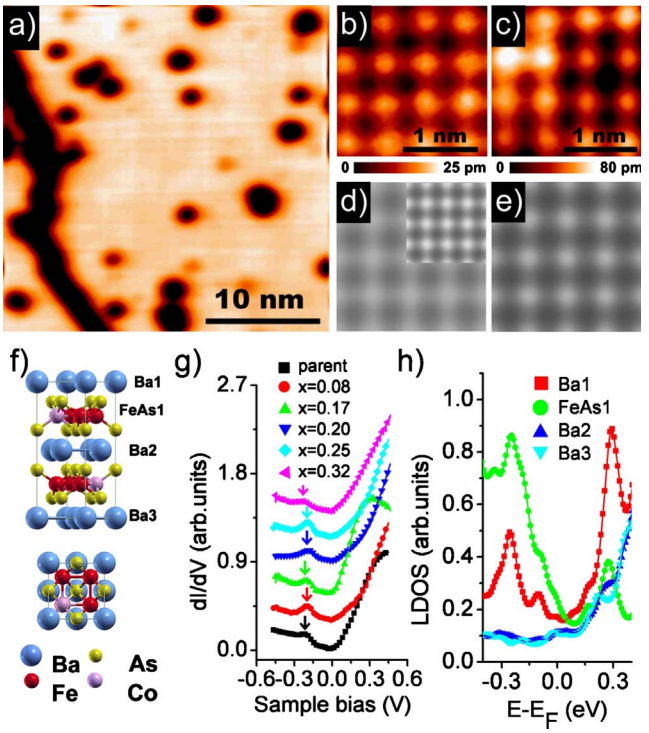

FIG. 1. (Color online) (a) Large-scale STM image of the $BaFe_{1.8}Co_{0.2}As_2$ surface with $\sqrt{2}\times\sqrt{2}$ structure (V_s=0.5 V,I=0.5 nA). (b) and (c) are STM images showing the $\sqrt{2}\times\sqrt{2}$ lattice with atomic resolution on the surfaces of $BaFe_2As_2$ (V_s=30 meV,I=3 nA) and $BaFe_{1.8}Co_{0.2}As_2$ (V_s=2 meV,I=20 nA), respectively. (d) and (e) are the simulated empty-state STM images with half Ba atoms on top of $BaFe_2As_2$ and $BaFe_{1.75}Co_{0.25}As_2$, respectively. (f) The side view and top view of the calculated structure of $BaFe_{1.75}Co_{0.25}As_2$. The calculated structure is orthorhombic in (d), and tetragonal in (e) and the inset of (d). (g) dI/dV spectroscopies for $BaFe_{2-x}Co_xAs_2$ with x=0, 0.08, 0.17, 0.20, 0.25, and 0.32, respectively. (h) Calculated LDOS for different layers in $BaFe_2As_2$. The layer definition is shown in (f).

structure (in the tetragonal notation). Our calculations are carried out by employing the Vienna *ab initio* simulation package (VASP) using the general gradient approximation with Perdew-Burke-Ernzerhof (PBE) functional and plane-wave-basis sets.[17–20] A supercell geometry with nine atomic layers (four FeAs layers and five Ba layers) and a vacuum layer about 30-Å thick are used to simulate the surface. The plane-wave cutoff is set to be 600 eV. For geometry optimization, we use a $4\times4\times1$ Monkhorst grid[21] to sample the Brillouin zone while a denser $6\times6\times1$ grid is used for density-of-states calculations. During the structural optimizations, we fix the bottom three (two Ba and one FeAs) layers in the bulk configuration and allow all other atoms in the supercell to move until all forces vanished within 0.02 eV/Å.

The simulated STM images for the parent with orthorhombic and tetragonal structures are displayed in Fig. 1(d), and both show squarelike pattern. No essential difference can be resolved from our simulation although the symmetries of the two structures diverge. It is reasonable considering that the distortion of the low-T orthormhombic structure from the high-T tetragonal structure in $BaFe_2As_2$ is quite minor.[22] The

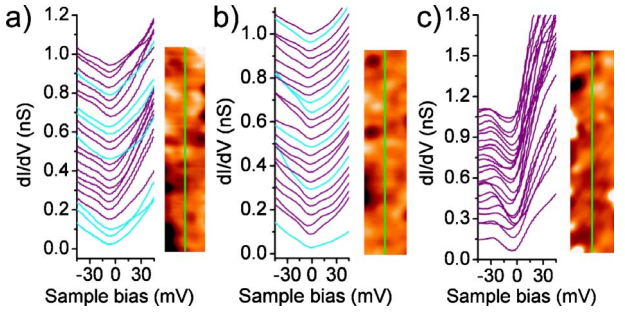

FIG. 2. (Color online) dI/dV spectroscopies measured along line trajectories on the $BaFe_{2-x}Co_xAs_2$ compounds with (a) x=0, (b) 0.20, (c) and 0.32. The tunneling setpoint for STS measurement is same (V_s=−0.1 V,I=0.5 nA). The lengths of the trajectories are 31, 32, and 28 nm, respectively. The gap feature is weaker in the blue (light gray) curves than in purple (dark gray) ones.

simulated STM image for x=0.25 (tetragonal structure) is shown in Fig. 1(e), which is similar to that of the parent compound. Orthorhombic distortion also has little effect on the simulated images. So the simulated STM images with half Ba-layer termination well reproduce the experimental data for both undoped and doped compounds. STM simulation for the parent compound with FeAs layer as the surface termination was also performed and only shows a squarelike lattice of 4 Å×4 Å (or 1×1 in the tetragonal notation). This is inconsistent with the observed STM images.

We calculated the local density of states (LDOS) of the parent for different layers and there is indeed a feature arising around −0.2 eV for the first Ba and FeAs layer, which is consistent with the STS results. That hump is absent in the LDOS of the inner Ba and FeAs layers. The agreement between experimental STM/STS results and theoretic simulations strongly suggests that the cleaved surface for the series of $BaFe_{2-x}Co_xAs_2$ compounds with x ranging from 0 to 0.32 is terminated by half layer of Ba atoms. The half Ba atoms form well-ordered $\sqrt{2}\times\sqrt{2}$ structure, which is insensitive to the orthorhombic structural distortion.

STS in narrower range around Fermi level was measured on the $\sqrt{2}\times\sqrt{2}$ surface for all the investigated compounds and the typical spatially resolved dI/dV spectroscopies for x=0, 0.20, and 0.32 are shown in Fig. 2. The dI/dV curves show a little bias asymmetry, especially for x=0.32, which could probably be due to the electron correlation effect.[23] Surprisingly a weak gap structure is generally observed, even for the parent compound. The gap size was defined by the kinks of the dip structure around Fermi level. The averaged gap size is 34 ± 6 meV for the parent, 28 ± 5 meV for x=0.20, and 38 ± 5 meV for x=0.32. We note that an energy gap 30–40 meV is also observed at the $\sqrt{2}\times\sqrt{2}$ surface of $SrFe_2As_2$.[13] STS was also measured on the striped surface for x=0.20 and the typical gap 2Δ is about 14 meV. It is close to that previously observed by STM (~12 meV) (Refs. 10 and 11) and ARPES (13 and 10 meV for different Fermi surfaces)[24] on such striped surface, which was attributed to the isotropic s-wave superconducting gap. The energy gap observed at the $\sqrt{2}\times\sqrt{2}$ surface is much larger than that at the striped surface, which indicates that the two surfaces diverge electronically. Occasionally gap feature be-

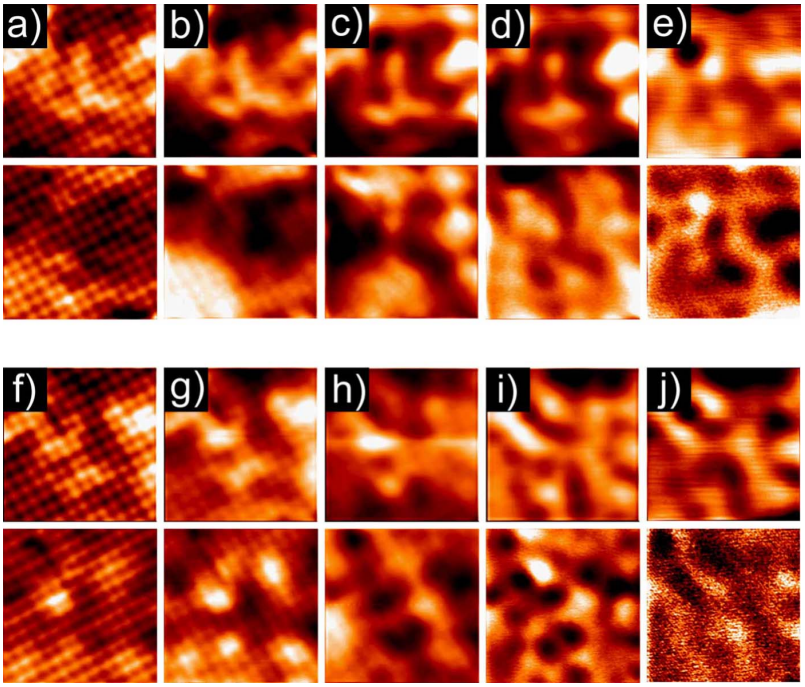

FIG. 3. (Color online) A series of topography images (upper) and corresponding dI/dV maps (lower) for $x=0.17$ measured at the same area with the size of 6.25×6.25 nm^2 when varying the tunneling parameters: (a) $V_s=0.02$ V and $I=2$ nA; (b) $V_s=0.02$ V and $I=0.5$ nA; (c) $V_s=0.05$ V and $I=0.5$ nA; (d) $V_s=0.1$ V and $I=0.5$ nA; (e) $V_s=0.4$ V and $I=0.5$ nA; (f) $V_s=-0.02$ V and $I=1.5$ nA; (g) $V_s=-0.02$ V and $I=0.5$ nA; (h) $V_s=-0.05$ V and $I=0.5$ nA; (i) $V_s=-0.1$ V and $I=0.5$ nA; and (j) $V_s=-0.4$ V and $I=0.5$ nA.

comes very weak at some random locations [blue (light gray) curves in Fig. 2]. But there seems no direct correlation between the STS and the topography by examining the site-dependent STS in Fig. 2.

The surface geometric and electronic structures differ from the bulk significantly, as evidenced by the $\sqrt{2}\times\sqrt{2}$ surface reconstruction and the calculated layer-dependent LDOS [Fig. 1(h)]. Consequently, the electron correlation might be different at the surface, which could be the reason why we did not observe the superconducting gap. The universality of the observed gap feature at the $\sqrt{2}\times\sqrt{2}$ surfaces suggests they might share the same origin. Bulk superconducting or spin density wave order can be excluded since the investigated compounds have different bulk collective orders. It could be the manifestation of a surface collective order induced by the new $\sqrt{2}\times\sqrt{2}$ surface termination. The observation of a universal gap feature indicates that the electronic correlation on the surfaces might depart substantially from the bulk and that the prediction of bulk properties based on surface-sensitive probes should be very careful. The gap feature is much stronger for the heavily doped samples, especially for $x=0.32$. The origin for such doping dependence is not clear and may be related to the correlation strength tuned by Co doping.

DI/dV mapping simultaneously with topography imaging was performed on all the investigated samples. Typical STM images and the corresponding dI/dV maps for $x=0.17$ are shown in Figs. 3(a) and 3(f) with sample bias of 0.02 and −0.02 V, respectively. The $\sqrt{2}\times\sqrt{2}$ lattice with atomic resolution is resolved in both topography and dI/dV images at such low tunneling-junction resistance. Furthermore, inhomogeneous corrugations at nanoscale are observed, superimposed on the square lattice. This is also evidenced in Figs. 1(b) and 1(c). If the tunneling current is lowered while the sample bias is unchanged, the atomic resolution becomes weaker as shown in Figs. 3(b) and 3(g) due to the increased distance between the tip and the substrate, while the nanoscale corrugations are still preserved. When the bias voltage is swept, the spatial inhomogeneity pattern in the same area also varies correspondingly and even reverses at some locations as clearly shown in Fig. 3. So the nanoscale inhomogeneity is unlikely to originate from topographic effect and should be due to electronic effect.

The larger-scale STM images and corresponding dI/dV maps for different doping concentrations are shown in Fig. 4. It is clear that the inhomogeneous charge modulation is a universal phenomenon, which is observed for all the compounds, including the parent compound, although it is relatively weak. The inhomogeneity pattern does not have spatial long-range order as indicated by the fast Fourier transform (FFT) (not shown) nor obvious preferable orientation. The evolution of the charge inhomogeneity as a function of the sample bias is also investigated. The spatial pattern and characteristic length of the charge inhomogeneity vary when the voltage is changed. We did autocorrelation calculation for the dI/dV images for quantitative analysis. The correlation lengths can be extracted from the radially integrated line profiles, which characterize the mean distance between the neighboring maxima/mimima.[25] Figure 4(j) shows the averaged correlation length depending on the doping level ($x=0.17$, 0.20, and 0.25) and energy. Surprisingly, the correlation length at a given energy and its evolution with energy is quite similar for different doping levels although they show different order and/or ordering strength in the bulk. This suggests that the charge modulation for different doping levels may share the same origin. The averaged correlation length is about 3.0 nm.

DFT calculation failed to reproduce such charge inhomogeneity in both the parent and doped compounds as shown in

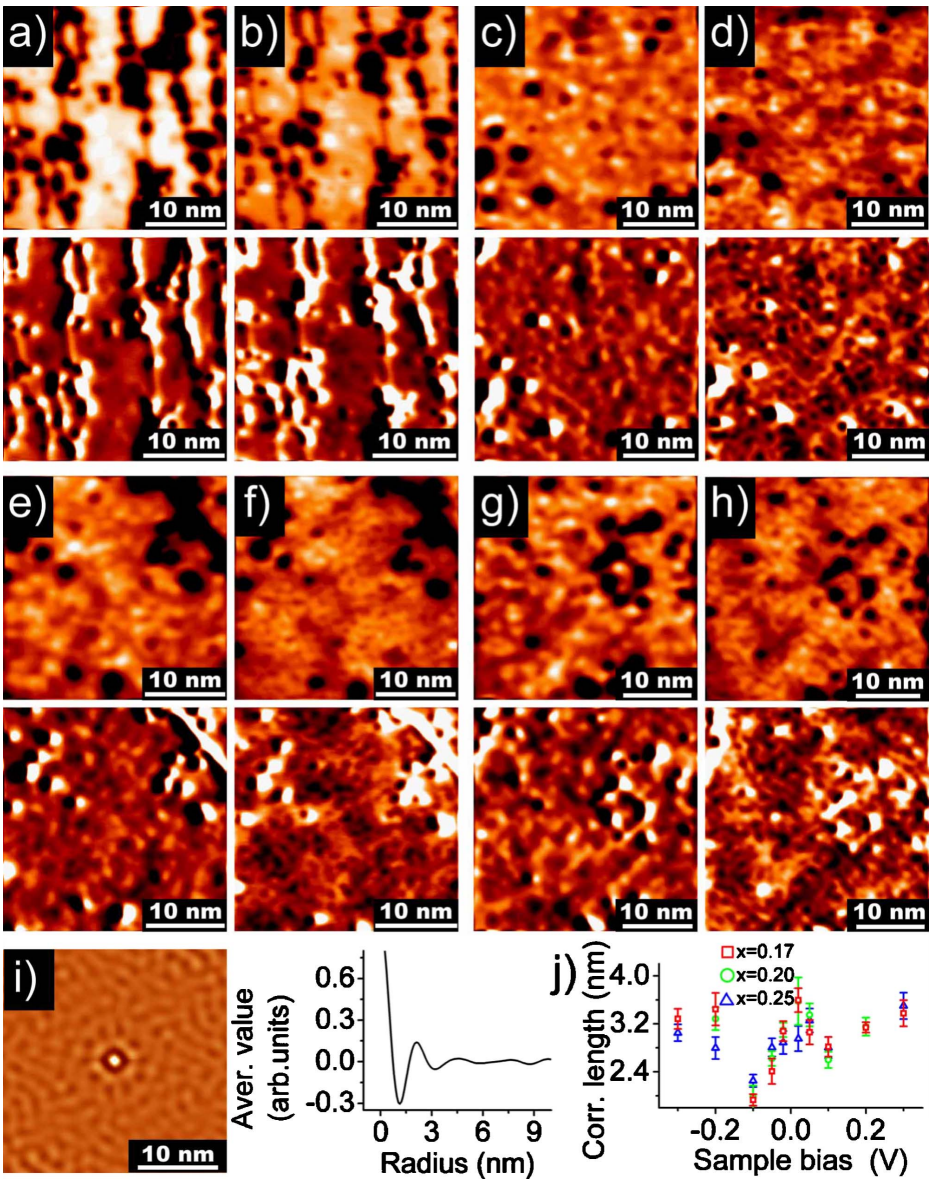

FIG. 4. (Color online) Large-scale topography (upper) and dI/dV (lower) images of $BaFe_{2-x}Co_xAs_2$ for (a) and (b) $x=0$, (c) and (d) 0.17, (e) and (f) 0.20, and (g) and (h) 0.25. The sample bias is 0.1 V for (a), (c), (e), and (g), and −0.1 V for (b), (d), (f), and (h). The tunneling current is 0.5 nA for all the images. The images for the same doping concentration are basically in the same area. (i) Autocorrelation image of the high-pass Fourier filtered dI/dV image in (d) and the corresponding radially integrated line profile. (j) Correlation length derived from the autocorrelation patterns of dI/dV images as a function of sample bias for $x=0.17$, 0.20, and 0.25. Each value is averaged over about ten measurements at different areas on the same sample.

Figs. 1(b) and 1(c). The electron interaction in iron pnictides is in the intermediate range,[26] where charge-density wave is strongly competitive with other collective orders,[27] and might dominate at the symmetry-broken $\sqrt{2}\times\sqrt{2}$ reconstructed surface. Quasiparticle interference (QPI) could also happen due to scattering from dopants or impurities. Since gap feature and charge modulation are both generally observed for all the investigated compounds, it is natural to think that they might be connected, e.g., the energy gap reflects the characteristic energy of a short-range charge order at the $\sqrt{2}\times\sqrt{2}$ surfaces. Further efforts are required to reveal its origin unambiguously.

For cuprates, spatially periodic charge modulations have been seen within the energy gap due to QPI oscillations in the superconducting state[28] or electronic order in the pseudogap state.[29,30] The periodicity is energy dependent for the former and independent for the latter. We acquired topography and dI/dV images with sample bias of −0.01 V within the energy gap as displayed in Fig. 5. The observed charge pattern does not show any long-range order.

IV. SUMMARY

In conclusion, a $\sqrt{2}\times\sqrt{2}$ surface structure terminated by half layer of Ba atoms is found to prevail at the surfaces of $BaFe_{2-x}Co_xAs_2$ compound with x varying from 0 to 0.32, which is insensitive to the orthorhombic distortion. Charge

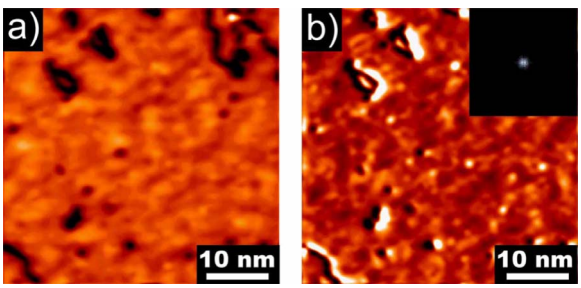

FIG. 5. (Color online) (a) Topography and (b) dI/dV images for $x=0.17$ at V_s of −0.01 V. The FFT of the dI/dV image is shown in the inset of (b).

inhomogeneity accompanied by an energy gap of around 30 meV appears at this $\sqrt{2}\times\sqrt{2}$ surface for all the investigated Co doping levels. The observed electronic effects strongly indicate that electron correlation at the symmetry-broken $\sqrt{2}\times\sqrt{2}$ surfaces might diverge from the bulk. It also sheds light on the exploration of cooperative effects of the correlated materials in reduced dimensions.

ACKNOWLEDGMENTS

We thank Zhenyu Zhang, Hanno H. Weitering, Dimitrie Culcer, and Donglai Feng for helpful discussions. This work was supported by NKBRPC (Grants No. 2009CB929502 and No. 2006CB922004), NSFC (Grants No. 10974188, No. 50532040, and No. 10825415), NCET, and CAS.

*cgzeng@ustc.edu.cn
†jlyang@ustc.edu.cn

[1] Y. Kamihara, T. Watanabe, M. Hirano, and H. Hosono, J. Am. Chem. Soc. **130**, 3296 (2008).
[2] H.-H. Wen, G. Mu, L. Fang, H. Yang, and X. Zhu, EPL **82**, 17009 (2008).
[3] X. H. Chen, T. Wu, G. Wu, R. H. Liu, H. Chen, and D. F. Fang, Nature (London) **453**, 761 (2008).
[4] G. F. Chen, Z. Li, D. Wu, G. Li, W. Z. Hu, J. Dong, P. Zheng, J. L. Luo, and N. L. Wang, Phys. Rev. Lett. **100**, 247002 (2008).
[5] Z.-A. Ren, G.-C. Che, X.-L. Dong, J. Yang, W. Lu, W. Yi, X.-L. Shen, Z.-C. Li, L.-L. Sun, F. Zhou, and Z.-X. Zhao, EPL **83**, 17002 (2008).
[6] M. Rotter, M. Tegel, and D. Johrendt, Phys. Rev. Lett. **101**, 107006 (2008).
[7] A. S. Sefat, R. Jin, M. A. McGuire, B. C. Sales, D. J. Singh, and D. Mandrus, Phys. Rev. Lett. **101**, 117004 (2008).
[8] K. Ishida, Y. Nakai, and H. Hosono, J. Phys. Soc. Jpn. **78**, 062001 (2009) and references therein.
[9] M. Boyer, K. Chatterjee, W. Wise, G. Chen, J. Luo, N. Wang, and E. Hudson, arXiv:0806.4400 (unpublished).
[10] F. Massee, Y. Huang, R. Huisman, S. de Jong, J. B. Goedkoop, and M. S. Golden, Phys. Rev. B **79**, 220517(R) (2009).
[11] Y. Yin, M. Zech, T. L. Williams, X. F. Wang, G. Wu, X. H. Chen, and J. E. Hoffman, Phys. Rev. Lett. **102**, 097002 (2009).
[12] V. B. Nascimento, A. Li, D. R. Jayasundara, Y. Xuan, J. O'Neal, S. Pan, T. Y. Chien, B. Hu, X. B. He, G. Li, A. S. Sefat, M. A. McGuire, B. C. Sales, D. Mandrus, M. H. Pan, J. Zhang, R. Jin, and E. W. Plummer, Phys. Rev. Lett. **103**, 076104 (2009).
[13] F. Niestemski, Vonbraun Nascimento, B. Hu, W. Plummer, J. Gillett, S. Sebastian, Z. Wang, and V. Madhavan, arXiv:0906.2761 (unpublished).
[14] F. Massee, S. de Jong, Y. Huang, J. Kaas, E. van Heumen, J. B. Goedkoop, and M. S. Golden, Phys. Rev. B **80**, 140507(R) (2009).
[15] X. F. Wang, T. Wu, G. Wu, R. H. Liu, H. Chen, Y. L. Xie, and X. H. Chen, New J. Phys. **11**, 045003 (2009).
[16] M. Gao, F. Ma, Z. Lu, and T. Xiang, arXiv:0909.5136 (unpublished).
[17] G. Kresse and D. Joubert, Phys. Rev. B **59**, 1758 (1999).
[18] G. Kresse and J. Furthmuller, Phys. Rev. B **54**, 11169 (1996).
[19] P. E. Blöchl, Phys. Rev. B **50**, 17953 (1994).
[20] J. P. Perdew, K. Burke, and M. Ernzerhof, Phys. Rev. Lett. **77**, 3865 (1996).
[21] H. J. Monkhorst and J. D. Pack, Phys. Rev. B **13**, 5188 (1976).
[22] Q. Huang, Y. Qiu, W. Bao, M. A. Green, J. W. Lynn, Y. C. Gasparovic, T. Wu, G. Wu, and X. H. Chen, Phys. Rev. Lett. **101**, 257003 (2008).
[23] K. Haule, J. H. Shim, and G. Kotliar, Phys. Rev. Lett. **100**, 226402 (2008).
[24] K. Terashima, Y. Sekiba, J. H. Bowen, K. Nakayama, T. Kawahara, T. Sato, P. Richard, Y.-M. Xu, L. J. Li, G. H. Cao, Z.-A. Xu, H. Ding, and T. Takahashi, Proc. Natl. Acad. Sci. U.S.A. **106**, 7330 (2009).
[25] J. L. Bubendorff, G. Garreau, S. Zabrocki, D. Berling, R. Jaafar, S. Hajjar, A. Mehdaoui, and C. Pirri, Surf. Sci. **603**, 373 (2009).
[26] Q. M. Si, E. Abrahams, J. H. Dai, and J.-X. Zhu, New J. Phys. **11**, 045001 (2009).
[27] V. Cvetkovic and Z. Tesanovic, Phys. Rev. B **80**, 024512 (2009); Z. Tesanovic (private communication).
[28] J. E. Hoffman, K. McElroy, D.-H. Lee, K. M. Lang, H. Eisaki, S. Uchida, and J. C. Davis, Science **297**, 1148 (2002).
[29] M. Vershinin, S. Misra, S. Ono, Y. Abe, Y. Ando, and A. Yazdani, Science **303**, 1995 (2004).
[30] T. Hanaguri, C. Lupien, Y. Kohsaka, D.-H. Lee, M. Azuma, M. Takano, H. Takagi, and J. C. Davis, Nature (London) **430**, 1001 (2004).